University of Groningen

Pronounced Environmental Effects on Injection Currents in EGaIn Tunneling Junctions Comprising Self-Assembled Monolayers

Carlotti, Marco; Degen, Maarten; Zhang, Yanxi; Chiechi, Ryan C.

[Link to publication in University of Groningen/UMCG research database](#)

Pronounced Environmental Effects on Injection Currents in EGaIn Tunneling Junctions Comprising Self-Assembled Monolayers

Marco Carlotti, Maarten Degen, Yanxi Zhang, and Ryan C. Chiechi*

Stratingh Institute for Chemistry & Zernike Institute for Advanced Materials, University of Groningen, Nijenborgh 4, 9747 AG Groningen, The Netherlands

S *Supporting Information*

ABSTRACT: Large-area tunneling junctions using eutectic Ga–In (EGaIn) as a top contact have proven to be a robust, reproducible, and technologically relevant platform for molecular electronics. Thus far, the majority of studies have focused on saturated molecules with backbones consisting mainly of alkanes in which the frontier orbitals are either highly localized or energetically inaccessible. We show that self-assembled monolayers of wire-like oligophenyleneethynylenes (OPEs), which are fully conjugated, only exhibit length-dependent tunneling behavior in a low-O_2 environment. We attribute this unexpected behavior to the sensitivity of injection current on environment. We conclude that, contrary to previous reports, the self-limiting layer of Ga_2O_3 strongly influences transport properties and that the effect is related to the wetting behavior of the electrode. This result sheds light on the nature of the electrode–molecule interface and suggests that adhesive forces play a significant role in tunneling charge-transport in large-area molecular junctions.
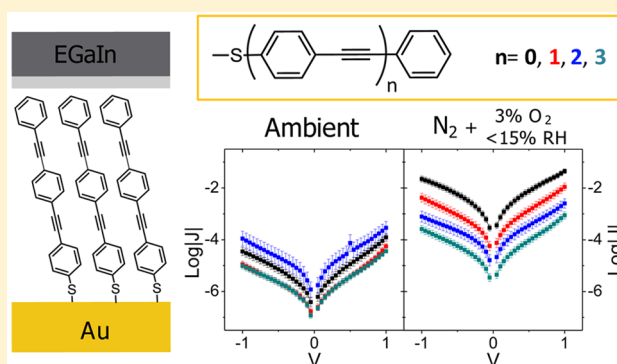
INTRODUCTION

This paper compares the electrical characteristics of large-area Au/SAM/EGaIn (eutectic Ga–In) molecular junctions comprising self-assembled monolayers (SAMs) of oligo(phenylene vinilene)s (OPEs) grown from mono- and bis-thioacetates in different environmental conditions. EGaIn is a liquid metal alloy that has, in recent years, been used in numerous applications in the fields of soft electronics and microfluidics.[1−4] Many of its interesting properties are related to a thin subnanometer layer of passivating Ga_2O_3, which EGaIn rapidly grows when exposed to air[5] and which confers the particular non-Newtonian rheological properties that make EGaIn useful.[6] In molecular electronics, EGaIn can be used to form stable, conformal, nondamaging contacts with SAMs[7] due to its ability to form sharp tips with a diameter of about 20 μm. These tips form macroscopic contacts to a SAM supported by a metal substrate enabling the formation of junctions in multiple areas of a substrate rapidly and reproducibly, allowing the collection of statistically significant data. Compared to single/few-molecules techniques, the stability of the junctions also allows more elaborate characterization of the electrical properties of the samples, e.g., via impedance spectroscopy.[8]

Since the dawn of molecular electronics, more than 40 years ago,[9,10] a wide variety of molecules has been investigated in molecular tunneling junctions of different configurations[11−13] to probe the effects of different structures and chemical functionalities on the flow of electrons. Most of the efforts have been directed toward techniques involving single- or few-

molecule junctions such as mechanically controlled and STM break junctions (MCBJ, STM-BJ) or conductive probe AFM (CP-AFM), respectively,[11] because results are relatively straightforward to model in silico;[12,14,15] yet, these experimental platforms do not readily translate to devices, which carry the practical constraints of needing to be integrated into a circuit and be reliable and reproducible.[16] Large-area junctions such as those comprising EGaIn, on the other hand, better resemble the possible architecture of an actual molecular electronic device.[11,17] Usually they make use of SAMs on metal electrodes as the active element and the template to define the unimolecular thickness of the junction in a bottom-up fashion.[18] Moreover, the use of SAMs can induce new properties of the tunneling systems which are not present when one or few molecules alone are investigated.[19]

Studies concerning large-area junctions typically make use of saturated thiols on coinage metals.[17,20,21] These SAMs are straightforward to prepare/acquire and are extensively characterized, and their transport characteristics are well-established; for these reasons they are often used as test beds.[13,17,22−27] Yet, the frontier orbitals are far from the Fermi level of the electrodes and do not strongly participate in the charge-transport across the junction. On the other hand, conjugated molecules, with more accessible frontier orbitals and the

possibility to interact with the electrode on the electronic level, have shown properties such a negative differential resistance,[28−33] conductance switching,[34−36] memory effects,[31] quantum interference,[37,38] and the ability to modify the Fermi energy and the electrostatics of the electrodes.[19,39,40] Polyphenylenes, OPEs, and similar conjugated structures have long been proposed as active elements in molecular electronics.[13,15,30,32,41−45] In particular, OPEs can be easily functionalized without distorting the conjugated backbone,[41,46−49] yet they are rarely investigated in large-area junctions.[20] This scarcity of experimental data may be due to difficulties in growing densely packed SAMs from rigid molecules with an extended π-system[21,38] or their sensitivity to oxidation; that is, saturated molecules are simply easier to handle.

One of the principal advantages of using thiols and coinage metals in molecular electronics is that Au is essentially inert and the Au−S bond is sufficiently strong to compete with advantageous adsorbates, however, the details of the surface chemistry of the Ga_2O_3 layer remain a mystery. Barber et al. studied the influence of the environment on the transport properties of saturated SAMs in Ag/SAM//EGaIn junctions (where / and // represent covalent and van der Waals contacts, respectively) and found no effect provided sufficient O_2 was present to form the Ga_2O_3 layer.[27] In an effort to facilitate working with sensitive π-conjugated molecules, we built an EGaIn measurement setup inside a large flowbox capable of maintaining a low-O_2 environment such that the Ga_2O_3 can form, but that sensitive compounds and SAMs can still be handled without appreciable oxidation. Surprisingly, we found a large influence of the environmental conditions on the electrical properties of junctions comprising SAMs of OPEs, in stark contrast to SAMs of alkanethiolates, which showed only a systematic shift in injection current.

■ RESULTS AND DISCUSSION

We first investigated the OPEs shown in Figure 1 under ambient conditions on template-stripped Au (Au^TS).[50] The
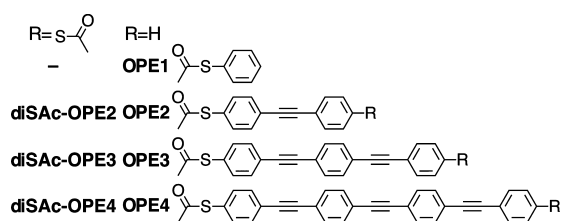

Figure 1. OPE compounds used to prepare self-assembled monolayers.

resulting data were characterized by unusually large dispersion, low current values, and low yield of working junctions, rendering them uninterpretable (Figure 2A). We then grew SAMs from the same compounds inside the flowbox from a toluene solutions using 1,8-diazabicyclo[5.4.0]undec-7-ene (DBU) as an in situ deprotecting agent (see Experimental Section) and measured them without any exposure to ambient conditions. These results are shown in Figure 2B; in an atmosphere of N_2 maintained at 1−3% O_2 and <15% relative humidity (RH), the yields of working junctions increased dramatically, the current-densities increased by approximately 2 orders of magnitude, and a clear length-dependence emerged.

Figure 3 shows a comparison of the histograms of log|J| at −0.5 V from SAMs prepared inside the flowbox and measured in the same controlled environment and under ambient conditions. Ambient data are characterized by broader histograms and by a systematically lower current. Although the peaks of the histograms shift somewhat, they do not follow an obvious trend. Flowbox data, however, yield narrow histograms with well-defined peaks that follow a clear trend in molecular length. Additionally, the yield of the nonshorting junctions increased from ∼75% in ambient to >90% in the flowbox. These data are summarized in Table 1.

We analyzed the data using a simplified version of Simmons' equation[51] (eq 1) for a more quantitative description of the electrical properties and to facilitate comparisons with studies of OPEs in other platforms. From the flowbox data we calculated a value of $\beta = 0.23 \pm 0.01$ Å^{-1} at 0.5 V using the theoretical end-to-end distances of the minimized geometries (Table S1.) This value is in agreement with theoretical predictions[15] and those reported by Lu et al.[52] and Kaliginedi et al.[42] using MCBJ and Liu et al.[53] using CP-AFM (Table 2). The same analysis was not possible with ambient data.

$$J = J_0 e^{-\beta d} \tag{1}$$

In addition to reporting a value of β, Lu et al. observed a change in the transport mechanism on going from **OPE1** to **OPE4** for Au/SAM/Au junctions comprising a series of bis-amino-terminated OPEs using STM-BJ and CP-AFM (though in the latter case the transition was not well-pronounced). A similar transition in the EGaIn junctions was reported more recently by Sangeeth et al.[56] for a series of oligo-(phenyleneimine) wires; in particular, they reported a transition from tunneling to hopping for junctions comprising molecules with a molecular backbone longer than 25−30 Å. In both cases, a hopping mechanism was distinguished via variable temperature conductance data; hopping is a thermally activated process that follows the Arrhenius reltionship, while tunneling does not depend on temperature.[57] To test for this transition in Au/SAM//EGaIn junctions we performed variable temperature studies on SAMs prepared in the flowbox and measured in microfluidic EGaIn junctions under an inert atmosphere. (Low-temperature measurements are incompatible with O_2 and H_2O vapor.) Figure 4 shows no dependence of conductance on temperature from which we conclude that there is no thermally activated process, and therefore, no tunneling to hopping transition.

The presence of some O_2 is necessary to form the self-limiting Ga_2O_3 skin responsible for the non-Newtonian behavior of EGaIn that permits it to retain sharp tips instead of relaxing to a Gaussian geometry.[6] Figure 5 shows tips formed in ambient and in the flowbox; 1−3% O_2 is sufficient to form tips in a reproducible fashion and collect reproducible data. While atomistic detail of the surface of EGaIn/Ga_2O_3 is currently experimentally inaccessible, the tips formed in the flowbox differ qualitatively from those formed in ambient. In particular, in the low-O_2, low-RH flowbox environment, EGaIn does not appear to wet the metal of the syringe needle, leading to the formation of a long column of liquid metal before the hourglass shape between the needle, and the surface ruptures to form the tips used for measurements. The tips formed inside the flowbox also appear sharper and smoother, and the surface shows less buckling compared to tips formed in ambient. The apparent sharpness does not necessarily affect the apex of the
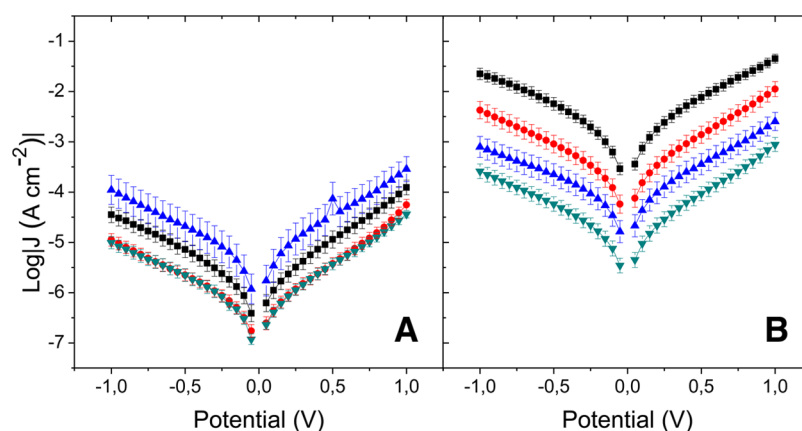
Figure 2. Semilog plot of J vs V for EGaIn/Ga$_2$O$_3$//OPE/Au^{TS} junctions: **OPE1** (black), **OPE2** (red), **OPE3** (blue), and **OPE4** (dark cyan). (A) Data collected in ambient conditions. (B) Data collected in a flowbox environment of N$_2$, 1−3% O$_2$ and RH < 15%. Error bars are per-junction confidence intervals calculated using $\alpha = 0.95$.
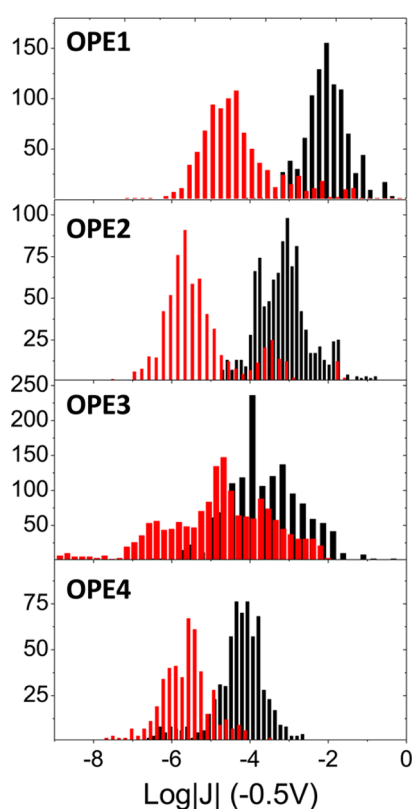

Figure 3. Histograms of all J/V data for **OPE1**, **OPE2**, **OPE3**, and **OPE4** in ambient (red) and in the flowbox environment (black) at −0.5 V. y-axes are counts. The histograms in ambient environment are broad, and the peak values show no obvious trend, while the histograms in the flowbox are sharp and the peaks follow a clear trend with molecular length.

tip, which is typically on the order of 20 μm in diameter. These are qualitative observations based on optical micrographs; however, we speculate that they could be due to a systematic difference in the wetting and/or mechanical properties of the Ga$_2$O$_3$ skin due to the different conditions under which they form. There is both a significantly reduced amount of O$_2$ and lower RH, and either or both could influence the kinetics and/ or thermodynamics of the formation of Ga$_2$O$_3$ and/or its chemical composition, crystal structure, surface states, electronic properties, thickness, etc.; it is a complex system,

Table 1. Summary of Electrical Data on SAMs of OPEs

measurement	compd			
	OPE1	OPE2	OPE3	OPE4
log|J| @ −0.5 V (flowbox) [A cm^{-2}]	−2.25	−3.04	−3.65	−4.24
log|J| @ −0.5 V (ambient) [A cm^{-2}]	−5.14	−5.65	−4.68	−5.65
yield of working junctions (flowbox) [%]	92	90	93	97
yield of working junctions (ambient) [%]	75	74	67	84

Table 2. Comparison of Values of β for OPEs Determined by Different Methods

ref	technique	atmosphere	β [Å^{-1}]
15	theoretical		0.25
54	theoretical		0.19
53	CP-AFM	ambient	0.20 ± 0.07
52	MCBJ	ambient	0.202 ± 0.002
42	MCBJ	inert	0.34 ± 0.01
55	STM^a	inert	0.32 ± 0.1
55	STM^b	inert	0.05 ± 0.01
this work	EGaIn	N$_2$ + 1−3% O$_2$, RH < 15%	0.23 ± 0.01

^{a}Thiol linkers. ^{b}Carbodithioate linkers.

and further study will be required to elucidate the exact mechanism. Irrespective of these microscopic details, there are clear qualitative differences in the tips of EGaIn and clear quantitative differences in the J/V characteristics of tunneling junctions comprising OPEs.

To confirm that the dramatic environmental effects seen with OPEs are not generalizable, we measured Ag^{TS}/SAM//EGaIn junctions comprising alkanethiolates in ambient conditions and in the flowbox environment. We chose these SAMs and Ag^{TS} substrates because they have been studied extensively in EGaIn junctions and are widely considered to be a benchmark in molecular electronics.[13,22,24−27] The resulting data are summarized in Table 3, revealing a systematic shift to lower values of log\|J\| and higher yields of working junctions in the flowbox compared to ambient conditions. There are two important findings: (i) a clear trend in log\|J\| with molecular length is present in both sets of data, and (ii) log\|J\| shifts in the opposite direction compared to the SAMs of OPEs.

Using eq 1, we calculated values of β for the series of alkanethiols: $\beta = 0.79 \pm 0.02$ and 0.71 ± 0.05 Å^{-1} in ambient
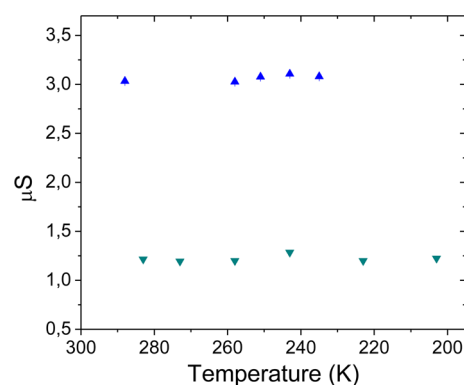
Figure 4. Arrhenius plots of low-bias conductance vs temperature for junctions comprising **OPE3** (blue ▲) and **OPE4** (dark cyan ▼). The invariance with temperature is characteristic of tunneling transport and indicates a lack of thermally activated processes. The low-bias conductance is reported as the slope of the J−V traces in the 0.1 V/ −0.1 V window. Data are shown down to the temperatures at which the majority of the junctions failed. Full J−V traces are shown in Figure S2.

Table 3. Summary of Electrical Data on SAMs of Alkanethiolates

	CH$_3$(CH$_2$)$_n$SH			
measurement	n = 9	n = 11	n = 13	n = 15
log|J| @ +0.5 V flowbox [A cm^{-2}]	−3.48	−4.10	−4.81	−5.95
log|J| @ +0.5 V ambient [A cm^{-2}]	−1.52	−2.44	−3.31	−4.82
yield of working junctions flowbox [%]	70	75	79	90
yield of working junctions ambient [%]	60	50	93	74
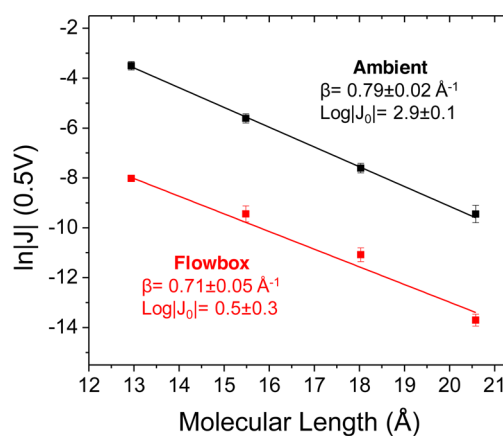
Figure 6. Plots of ln J @ +0.5 V vs molecular length in Å for Ag^{TS}/ SAM//EGaIn junctions comprising CH$_3$(CH$_2$)$_9$SH, CH$_3$(CH$_2$)$_{11}$SH, CH$_3$(CH$_2$)$_{13}$SH, and CH$_3$(CH$_2$)$_{15}$SH. The data collected in the flowbox environment (N$_2$ atmosphere with 1−3% O$_2$, RH < 15%) are reported in red, while those obtained in ambient conditions are in black. Error bars are per-junction confidence intervals calculated using α = 0.95. The straight lines are linear fits of the data.

and flowbox conditions, respectively, in perfect agreement with literature values (acquired under ambient conditions).[25,58] These data are plotted in Figure 6; there is a negligible change to the distance-dependence, strongly suggesting that the transport mechanism is insensitive to environmental conditions for alkanethiols.[14] There is, however, a difference in the values of J_0, which appears to be larger for the measurements performed in ambient conditions (i.e., the contact resistance increases in the flowbox). Simeone et al. reported a value of log\| J_0[A cm^{-2}]\| = 3.6 ± 0.3 @ 0.5 V for Ag^{TS}/SAM//EGaIn junctions in ambient conditions.[25] We found log\|J_0[A cm^{-2}]\| = 2.9 ± 0.1 in ambient conditions and log\|J_0[A cm^{-2}]\| = 0.5 ± 0.3 in the flowbox. That the injection current, J_0, is 3 orders of magnitude lower in the flowbox, yet the decay constant, β, is unaffected, suggests that the environmental effects on SAMs of alkanethiolates are confined to an interface. Also, since the Ag^{TS}/SAM and Au^{TS}/SAM interfaces do not change between ambient and flowbox conditions, it is reasonable to assume that the effects of a low-O$_2$, low-RH are confined to the SAM// EGaIn interface and that the effects of the different environments are affecting the formation/properties of the Ga$_2$O$_3$ layer. This hypothesis is consistent with the observation that the same substrate measured first in the flowbox and then in

ambient and then measured again in the flowbox will exhibit the characteristic histograms shown in Figure 3 in the respective environments (Figure S4). The effect, however, does not reduce to an increase in contact resistance in a low-N$_2$, low-RH atmosphere because SAMs of OPEs can only be measured in the flowbox, where the values of J increase compared to ambient conditions, *lowering* the contact resistance. An alternative hypothesis is simply that the differences in the geometries of the tips introduces a systematic underestimation of the areas of the junctions in the flowbox (and/or an overestimation in ambient), but the differences in
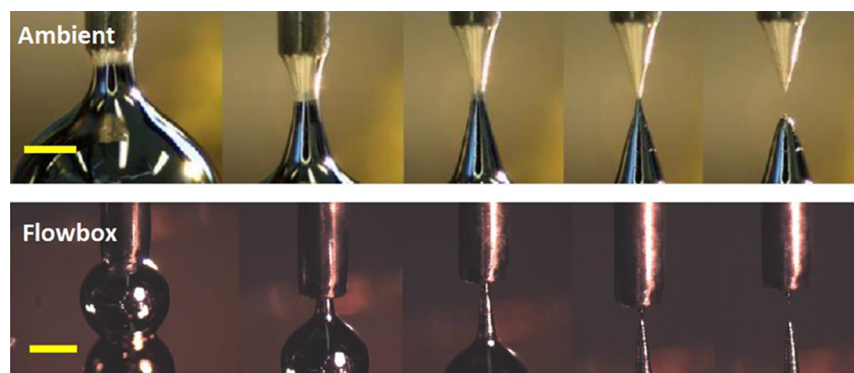

Figure 5. Formation of tips of EGaIn in ambient conditions (top) and in a flowbox kept at 2.5% O$_2$, RH < 15% (bottom). The yellow scale bar is 500 μm. Although the process of necking into an hourglass shape and severing into sharp tips is the same in both cases, in the flowbox EGaIn does not wet the metallic syringe needle.

the magnitude in J would require a systematic error in the measured diameters of a factor of 5−15 between the flowbox and ambient conditions. That hypothesis is also unable to explain the inability to resolve a length-dependence from OPEs or the commensurate broadening of the histograms in ambient conditions.

Barber et al. studied the effects of the composition of the atmosphere on Au^{TS}/SAM//EGaIn junctions comprising aliphatic SAMs and found negligible effects for dodecanethiol and 12-thiododecanoic acid as well as for alkanethiols.[27] Their methodology differed somewhat from ours; the tips used to form the junctions were prepared in air or pure O_2 before being transferred in different environments, while we prepared the SAMs, formed the tips, and performed the measurements in either ambient or in the flowbox. Thus, our observation that there is a negligible effect on β for SAMs of alkanethiolates is consistent as well as our observation that SAMs of OPEs are affected dramatically and that J_0 is affected for SAMs of alkanethiolates.

To explore the hypothesis that the environmental effects can be ascribed to the SAM//EGaIn interface, we measured SAMs formed from symmetric dithioacetate (diSAc) derivatives of **OPE2**, **OPE3**, and **OPE4** (denoted **diSAc-OPE2**, **diSAc-OPE3**, and **diSAc-OPE4**, respectively) in Au^{TS}/SAM//EGaIn junctions in ambient conditions and in the flowbox. (**diSAc-OPE1** does not form densely packed, upright SAMs.) Figure 7 clearly shows that the same environmental effect is present for this series; a trend in J molecular length is evident only when the molecules are measured in the controlled atmosphere of the flo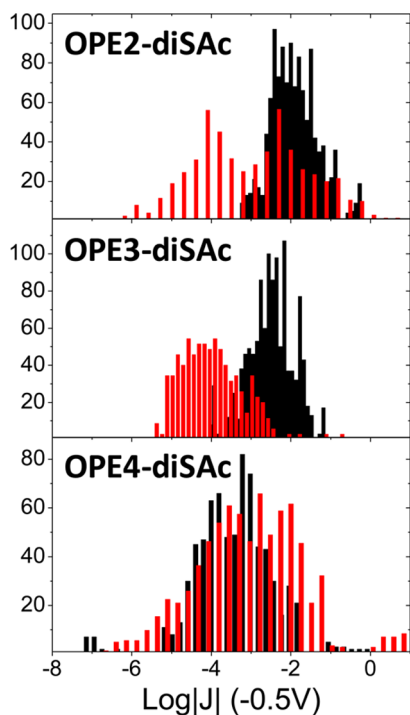wbox, but it collapses when the same experiments are performed in ambient conditions. The *in situ* deprotection procedure results in predominantly free thiol (SH) groups at the SAM//EGaIn interface, with some residual thioacetate ($SC(O)CH_3$) groups.[21] Thus, the interaction is chemically very different than for the OPE series, which presents a bare phenyl group. Thiols, by comparison, have a higher surface free-energy (lower contact angle with water) and can be considered more strongly interacting by virtue of the lone pairs of the sulfur atoms present at the SAM//EGaIn interface for the diSAc-OPE series, yet the data acquired from SAMs of diSAc-OPEs and OPEs in ambient conditions are virtually indistinguishable.

The values of $\log|J|$ acquired in the flowbox show clear length-dependence and are systematically higher for the diSAc-OPE series as compared to the (mono-diSAc) OPE analogues, meaning that there is a higher injection current (and lower contact resistance) when a thiol is present at the SAM//EGaIn interface; $\log|J_0[A\ cm^{-2}]| = -1.6 \pm 0.1$ and $\log|J_0[A\ cm^{-2}]| = -0.3 \pm 0.3$ for the mono-SAc and diSAc OPEs, respectively. Using eq 1, we found $\beta = 0.23 \pm 0.01$ Å^{-1} and $\beta = 0.23 \pm 0.05$ Å^{-1} for the OPE and diSAc-OPE series, respectively (Figure 8).
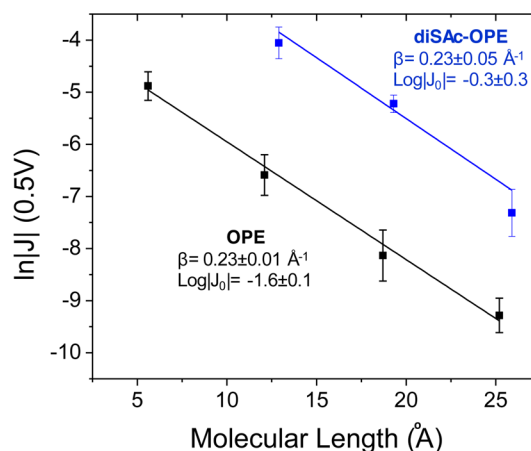

Figure 8. Plots of ln $|J|$ @0.5 V vs molecular length in Å for Au^{TS}/SAM//EGaIn junctions formed from mono- (black) and di- (red) thioacetate derivatives of OPEs of varying length in the flowbox environment (structures are shown in Figure 1). Error bars are per-junction confidence intervals calculated using $\alpha = 0.95$. The straight lines are linear fits of the data.

Thus, modifying the SAM//EGaIn interface chemically and measuring SAMs of OPEs in the flowbox affects the J/V data analogously to changing the environment for SAMs of alkanethiols without altering the SAM//EGaIn interface chemically. This observation further supports the hypothesis that the Ga_2O_3 layer present at the surface of EGaIn is affected by the environment; however, this interface does not appear to be more strongly coupled to the SAM in the flowbox since chemically increasing the interaction between the SAM and EGaIn mimics the effect of measuring SAMs of alkanethiolates in ambient conditions. That is, the difference between a Ph-H and Ph-SH interface is analogous to Ga_2O_3 prepared in flowbox and ambient conditions, respectively.

In the absence of the ability to acquire experimental data on the atomistic details of the oxide layer, we can estimate the influence of the low-O_2 atmosphere by considering the thermodynamics and kinetics. The change in the free-energy of formation of Ga_2O_3 is negligible; $\Delta_r G$ goes from −998 kJ mol^{-1} under ambient conditions to roughly −981 at 1% O_2.[59]

Figure 7. Histograms of all J/V data for **diSAc-OPE2** (top), **diSAc-OPE3** (middle), and **diSAc-OPE4** (bottom) in ambient (red) and in the flowbox environment (black; N_2 atmosphere with 1−3% O_2, RH < 15%) at −0.5 V. y-axes are counts. The data acquired in air and characterized by broad distributions with no obvious trend while the data acquired in the flowbox are distributed more narrowly and the peak values follow a clear trend with molecular length.

Also, the frequency of collisions between O_2 molecules and the surface of EGaIn at 1% O_2 is on the order of 10^{15} s^{-1}, excluding O_2 as a rate-limiting step in the formation of the oxide (assuming a conical tip with diameter of 0.5 mm, a height of 1 mm and perfect gas behavior of O_2). Finally, the non-Newtonian properties of EGaIn are retained in the flowbox with oxygen levels as low as 300 ppm, although under such conditions the reproducible formation of tips becomes prohibitively difficult. Doudrick et al. reported that in the case of Galistan (a Ga/In/Sn ternary liquid alloy) a partial-pressure of O_2 of 0.03 mPa is sufficient for the oxide to form.[60] Thus, we are confident that the thickness of the surface of EGaIn/Ga_2O_3 is unaffected by the reduction in O_2. It is also unlikely that the effect originates entirely from RH, as it varies seasonally and geographically and EGaIn junctions have been studied year-round and on at least three continents.[18,27] It is possible that surfaces of EGaIn/Ga_2O_3 formed in a controlled atmosphere may have a different contact resistance because they are free of contaminants and dopants from the ambient environment;[61] however, that explanation is inconsistent with experiments that find SAM/EGaIn interfaces formed in ambient conditions comparable to SAM//Au[62] and molecule/Au[63] interfaces. Although we cannot rule out a microscopic difference in the surface of the EGaIn tip affecting a change in effective contact area, we can exclude the possibility that such error is systematic. We performed conductivity measurements using the EGaIn tips formed identically to those used to measure SAMs on an n-doped Si wafer bearing a native oxide (cleaned with O_2 plasma) and exfoliated highly oriented pyrolytic graphite (HOPG). In ambient conditions, the conductivity (at −0.5 V) was a factor of 2 and 6 times higher than in the flowbox for Si and HOPG, respectively. The differences in J for SAMs of alkenthiolates are on the order of 100, and therefore, experimental error in determining the effective contact area is not responsible for the difference in J_0. The effects on J_0 (and presumably on the ability to measure SAMs of OPEs) are specific to SAMs of alkanethiolates and do not reduce to a difference in the geometry/topology of the tip.

Given that the environmental effects are localized to the SAM//EGaIn interface and that they cannot be ascribed to a thinner or chemically different Ga_2O_3 layer altering the coupling and/or contact resistance and that the differences in injection currents cannot be explained by experimental error in the determination of the area of the junction, we conclude that the effects can be ascribed to a difference in wetting. The qualitative differences in the tips shown in Figure 5 suggest very different wetting behavior of EGaIn (but probably not the SAMs, see Figure S5) in different environments. This difference could lead to differences in the mechanical stresses at the SAM/EGaIn interface arising from adhesive forces; a "gentler" contact may be necessary to measure fragile SAMs of OPEs. Likewise, such a contact could explain the increase in the yields of working junctions and increased injection currents of SAMs of alkanethiolates. Moreover, increasing the surface free-energy of SAMs of OPEs by introducing thiol groups mimics the behavior of measuring SAMs of alkanethiols in ambient conditions, which is consistent with the hypothesis that injection currents scale with wetting and that tips of EGaIn formed in ambient conditions wet SAMs better than those prepared in the flowbox.

CONCLUSIONS

The environment under which SAMs and junctions of large-area Au^{TS}/SAM//Ga_2O_3/EGaIn junctions comprising SAMs of mono- and dithiol OPEs and Ag^{TS}/SAM//Ga_2O_3/GaIn junctions comprising SAMs of alkanethiolates are formed has a pronounced, systematic effect on tunneling charge-transport. The resistance of SAMs of OPEs decreases in low-O_2, low-humidity environments, while the resistance of SAMs of alkanethiolates increases. The quantifiable effect is the injection current of the latter; SAMs of mono- and dithiol OPEs do not produce meaningful trends under ambient conditions. By comparing SAMs of OPEs that present either a bare phenyl group (Ph) or a thiophenol group (Ph-SH) to the EGaIn interface and SAMs of alkanethiolates under ambient conditions and a controlled atmosphere of N_2 with 1−3% O_2 and RH < 15%, we unambiguously ascribe the effects to the nature of the SAM/Ga_2O_3; injection currents (J_0), but not decay constants (β), are influenced by the environment under which measurements are performed and by the chemistry of the interface. Variable temperature measurements establish the mechanism of transport through OPEs, which can only be measured at low-O_2 and low-RH, as tunneling.

This work identifies the wetting properties of the SAM//Ga_2O_3/EGaIn interface as a critical component that can become limiting in the case for π-conjugated molecules with small values of β (relative to n-alkanes). This observation may also explain the statistical variance of injection currents of SAMs of alkanethiolates measured with EGaIn. The ability to adjust the injection current sufficiently to measure conjugated molecules underscores the universality of EGaIn as a top contact for the formation of large-area tunneling junctions and enables future studies on more exotic molecular systems.

EXPERIMENTAL SECTION

Flowbox. The flowbox was realized using a Terra Universal stainless steel glovebox series 400 SS (60 in. × 33 in. × 37 in.) equipped with a Dual Purge flow regulator (Terra Universal) connected to the house nitrogen. To keep the levels of O_2 and RH under established limits (3% and 15%, respectively), the flow regulator was connected to a NitroWatch RH controller equipped with a Humex Sensor (Terra Universal) and to an oxygen analyzer (Illinois Instruments model 810). The nitrogen flow was kept at approximately 0.25 L min^{-1} when the box was not used (to preserve the atmosphere inside) and was increased to 2.4 L min^{-1} during the measurements and the handling of chemicals and substrates. The entire EGaIn measurement setup was housed inside the flowbox.

Materials. Benzenethiol (**OPE1**), 1-decanethiol (**C10SH**), 1-dodecanethiol (**C12SH**), 1-tetradecanethiol (**C14SH**), and 1-hexadecanethiol (**C16SH**) were obtained from Sigma-Aldrich and purified by column cromatography (silica, hexane) with the excaption of **OPE1** which was used as received. The synthesis of **OPE2**, **OPE3**, **diSAc-OPE2**, **diSAc-OPE3**, and **diSAc-OPE4** is described elsewhere.[42] All compounds were stored in nitrogen-flushed vials and in the dark. Their structures were verified by acquiring ^1H NMR and IR spectra immediately prior to use and comparing them with the spectra acquired immediately after purification. **OPE4** was prepared starting from 1-ethynyl-4-((4-(phenylethynyl)phenyl)ethynyl)benzene as described in the Supporting Information.

SAM Formation. SAMs of the OPE series compounds were formed by incubating the thioacetate precursors with 1 × 1 cm^2

template-stripped Au surfaces (100 nm-thick) overnight in 3 mL of 50 μM solution of the respective compound in freshly distilled toluene followed by addition of 0.05 mL of 17 mM diazabicycloundec-7-ene (DBU) solution in toluene 1 h prior to the measurement. The substrates were then rinsed with ethanol and left to dry for 15 min. This procedure was used for both mono- and di-SAc terminated OPEs and performed in the flowbox controlled environment. SAMs of alkanethiols on Ag^{TS} (200 nm thick, 1×1 cm^2 surface) were grown from 3 mM solutions of the respective alkanethiol in degassed EtOH overnight; they were then rinsed and dried as previously described. More information can be found in the Supporting Information. Sample preparation and handling were performed in a nitrogen flowbox with a controlled O$_2$ level between 1% and 3% (some O$_2$ is necessary to form tips of EGaIn) and humidity below 10%, in the case of the OPE series, both mono-SAc and di-SAc, and the alkanethiol series measured in the low-O$_2$ environment.

EGaIn J–V Measurement. EGaIn measurements were carried on two identical setups, one positioned on a laboratory bench (ambient conditions) and one positioned in the flowbox described above. The details of the EGaIn setup are described elsewhere.[38] For each compound, 3–4 substrates were prepared, and at least 15 Au^{TS}/SAM//Ga$_2$O$_3$/EGaIn junctions per sample were measured (10 scans from 0 V → 1 V → −1 V → 0 V, steps of 0.05 V) for a total of at least 450 traces per SAM for the OPE series and at least 100 for the alkanethiols. A new EGaIn tip was prepared every 5–8 junctions and flattened by gently pushing it on a Si wafer a few times according to the procedure reported by Simeone et al.[25]

J–V Data Processing. Data were acquired as described and then parsed in a "hands-off" manner using Scientific Python to produce histograms of J for each value of V and the associated Gaussian fits (using a least-squares fitting routine). The confidence intervals for $\mu_{\log J}$ (Gaussian mean) depicted as error bars in the J–V plots were calculated using $\alpha = 0.95$ from $\sigma_{\log J}$ (standard deviation) taken from Gaussian fits and a number of degrees of freedom equal to the number of junctions − 1. The number of traces used for the statistical analysis can be found in the Supporting Information.

Ellipsometry. The SAMs were characterized by ellipsometry. These measurements were acquired on fresh samples in air on a V-Vase Rotating Analyzer equipped with a HS-190 monochromator ellipsometer and calculated via a two-layer model consisting of a bottom Au layer, for which optical constants were calculated from freshly prepared template-stripped Au surfaces, and a Cauchy layer with a chosen value of $n = 1.5$ and $k = 0$ at all wavelengths ($A = 1.5$, $B = C = 0$).[21]

ASSOCIATED CONTENT

Ⓢ Supporting Information

The Supporting Information is available free of charge on the ACS Publications website at DOI: 10.1021/acs.jpcc.6b07089.

> Full description of the synthesis and characterization of new compounds, details of the electrical measurements, and raw variable temperature data (PDF)

AUTHOR INFORMATION

Corresponding Author
*E-mail: r.c.chiechi@rug.nl.
Notes
The authors declare no competing financial interest.

REFERENCES

(1) Khan, M. R.; Eaker, C. B.; Bowden, E. F.; Dickey, M. D. Giant and Switchable Surface Activity of Liquid Metal via Surface Oxidation. *Proc. Natl. Acad. Sci. U. S. A.* **2014**, *111*, 14047−14051.

(2) Khan, M. R.; Trlica, C.; Dickey, M. D. Recapillarity: Electrochemically Controlled Capillary Withdrawal of a Liquid Metal Alloy From Microchannels. *Adv. Funct. Mater.* **2015**, *25*, 671−678.

(3) Tang, S.-Y.; Lin, Y.; Joshipura, I. D.; Khoshmanesh, K.; Dickey, M. D. Steering Liquid Metal Flow in Microchannels Using Low Voltages. *Lab Chip* **2015**, *15*, 3905−3911.

(4) Wu, Z.; Hjort, K.; Jeong, S. H. Microfluidic Stretchable Radio-Frequency Devices. *Proc. IEEE* **2015**, *103*, 1211−1225.

(5) Cademartiri, L.; Thuo, M. M.; Nijhuis, C. A.; Reus, W. F.; Tricard, S.; Barber, J. R.; Sodhi, R. N. S.; Brodersen, P.; Kim, C.; Chiechi, R. C.; et al. Electrical Resistance of Ag^{TS}−S(CH$_2$)$_{N−1}$CH$_3$//Ga$_2$O$_3$/EGaIn Tunneling Junctions. *J. Phys. Chem. C* **2012**, *116*, 10848−10860.

(6) Dickey, M. D.; Chiechi, R. C.; Larsen, R. J.; Weiss, E. A.; Weitz, D. A.; Whitesides, G. M. Eutectic Gallium-Indium (EGaIn): A Liquid Metal Alloy for the Formation of Stable Structures in Microchannels at Room Temperature. *Adv. Funct. Mater.* **2008**, *18*, 1097−1104.

(7) Chiechi, R.; Weiss, E.; Dickey, M.; Whitesides, G. Eutectic Gallium-Indium (EGaIn): A Moldable Liquid Metal for Electrical Characterization of Self-Assembled Monolayers. *Angew. Chem., Int. Ed.* **2008**, *47*, 142−144.

(8) Jiang, L.; Sangeeth, C. S. S.; Nijhuis, C. A. The Origin of the Odd-Even Effect in the Tunneling Rates Across EGaIn Junctions With Self-Assembled Monolayers (SAMs) of N-Alkanethiolates. *J. Am. Chem. Soc.* **2015**, *137*, 10659−10667.

(9) Aviram, A.; Ratner, M. A. Molecular Rectifiers. *Chem. Phys. Lett.* **1974**, *29*, 277−283.

(10) Mann, B.; Kuhn, H. Tunneling Through Fatty Acid Salt Monolayers. *J. Appl. Phys.* **1971**, *42*, 4398−4405.

(11) Wang, G.; Kim, T.-W.; Lee, T. Electrical Transport Characteristics Through Molecular Layers. *J. Mater. Chem.* **2011**, *21*, 18117−18136.

(12) Leary, E.; La Rosa, A.; Gonzalez, M. T.; Rubio-Bollinger, G.; Agrait, N.; Martin, N. Incorporating Single Molecules Into Electrical Circuits. The Role of the Chemical Anchoring Group. *Chem. Soc. Rev.* **2015**, *44*, 920−942.

(13) Metzger, R. M. Unimolecular Electronics. *Chem. Rev.* **2015**, *115*, 5056−5115.

(14) Khoo, K. H.; Chen, Y.; Li, S.; Quek, S. Y. Length Dependence of Electron Transport Through Molecular Wires - A First Principles Perspective. *Phys. Chem. Chem. Phys.* **2015**, *17*, 77−96.

(15) Nishizawa, S.; Hasegawa, J.-y.; Matsuda, K. Theoretical Investigation of the ß Value of the Π-Conjugated Molecular Wires by Evaluating Exchange Interaction Between Organic Radicals. *J. Phys. Chem. C* **2013**, *117*, 26280−26286.

(16) Bergren, A. J.; Zeer-Wanklyn, L.; Semple, M.; Pekas, N.; Szeto, B.; McCreery, R. L. Musical Molecules: The Molecular Junction as an Active Component in Audio Distortion Circuits. *J. Phys.: Condens. Matter* **2016**, *28*, 094011.

(17) Akkerman, H. B.; Blom, P. W. M.; de Leeuw, D. M.; de Boer, B. Towards Molecular Electronics With Large-Area Molecular Junctions. *Nature* **2006**, *441*, 69−72.

(18) Zhang, Y.; Zhao, Z.; Fracasso, D.; Chiechi, R. C. Bottom-Up Molecular Tunneling Junctions Formed by Self-Assembly. *Isr. J. Chem.* **2014**, *54*, 513−533.

(19) Kovalchuk, A.; Abu-Husein, T.; Fracasso, D.; Egger, D. A.; Zojer, E.; Zharnikov, M.; Terfort, A.; Chiechi, R. C. Transition Voltages Respond to Synthetic Reorientation of Embedded Dipoles in Self-Assembled Monolayers. *Chem. Sci.* **2016**, *7*, 781−787.

(20) Kronemeijer, A. J.; Huisman, E. H.; Akkerman, H. B.; Goossens, A. M.; Katsouras, I.; van Hal, P. A.; Geuns, T. C. T.; van der Molen, S. J.; Blom, P. W. M.; de Leeuw, D. M. Electrical Characteristics of Conjugated Self-Assembled Monolayers in Large-Area Molecular Junctions. *Appl. Phys. Lett.* **2010**, *97*, 173302.

(21) Valkenier, H.; Huisman, E. H.; van Hal, P. A.; de Leeuw, D. M.; Chiechi, R. C.; Hummelen, J. C. Formation of High-Quality Self-Assembled Monolayers of Conjugated Dithiols on Gold: Base Matters. *J. Am. Chem. Soc.* **2011**, *133*, 4930−4939.

(22) Yoon, H. J.; Bowers, C. M.; Baghbanzadeh, M.; Whitesides, G. M. The Rate of Charge Tunneling Is Insensitive to Polar Terminal Groups in Self-Assembled Monolayers in $Ag^{TS}S(CH_2)_nM(CH_2)_mT//Ga_2O_3/EGaIn$ Junctions. *J. Am. Chem. Soc.* **2014**, *136*, 16−19.

(23) Bowers, C. M.; Liao, K.-C.; Zaba, T.; Rappoport, D.; Baghbanzadeh, M.; Breiten, B.; Krzykawska, A.; Cyganik, P.; Whitesides, G. M. Characterizing the Metal-SAM Interface in Tunneling Junctions. *ACS Nano* **2015**, *9*, 1471−1477.

(24) Jiang, L.; Sangeeth, C. S. S.; Wan, A.; Vilan, A.; Nijhuis, C. A. Defect Scaling With Contact Area in EGaIn-Based Junctions: Impact on Quality, Joule Heating, and Apparent Injection Current. *J. Phys. Chem. C* **2015**, *119*, 960−969.

(25) Simeone, F. C.; Yoon, H. J.; Thuo, M. M.; Barber, J. R.; Smith, B.; Whitesides, G. M. Defining the Value of Injection Current and Effective Electrical Contact Area for EGaIn-based Molecular Tunneling Junctions. *J. Am. Chem. Soc.* **2013**, *135*, 18131−18144.

(26) Engelkes, V. B.; Beebe, J. M.; Frisbie, C. D. Length-Dependent Transport in Molecular Junctions Based on SAMs of Alkanethiols and Alkanedithiols: Effect of Metal Work Function and Applied Bias on Tunneling Efficiency and Contact Resistance. *J. Am. Chem. Soc.* **2004**, *126*, 14287−14296.

(27) Barber, J. R.; Yoon, H. J.; Bowers, C. M.; Thuo, M. M.; Breiten, B.; Gooding, D. M.; Whitesides, G. M. Influence of Environment on the Measurement of Rates of Charge Transport Across $Ag^{TS}/SAM//Ga_2O_3/EGaIn$ Junctions. *Chem. Mater.* **2014**, *26*, 3938−3947.

(28) Perrin, M. L.; Frisenda, R.; Koole, M.; Seldenthuis, J. S.; Gil, J. A. C.; Valkenier, H.; Hummelen, J. C.; Renaud, N.; Grozema, F. C.; Thijssen, J. M.; et al. Large Negative Differential Conductance in Single-Molecule Break Junctions. *Nat. Nanotechnol.* **2014**, *9*, 830−834.

(29) Kim, S.-U.; Shin, H.-K.; Kwon, Y.-S. Study on the Negative Differential Resistance Properties of Self-Assembled Organic Thin Films by Using STM. *Colloids Surf., A* **2005**, *257−258*, 211−214.

(30) Fan, F.-R. F.; Yao, Y.; Cai, L.; Cheng, L.; Tour, J. M.; Bard, A. J. Structure-Dependent Charge Transport and Storage in Self-Assembled Monolayers of Compounds of Interest in Molecular Electronics: Effects of Tip Material, Headgroup, and Surface Concentration. *J. Am. Chem. Soc.* **2004**, *126*, 4035−4042.

(31) Tour, J. M.; Rawlett, A. M.; Kozaki, M.; Yao, Y.; Jagessar, R. C.; Dirk, S. M.; Price, D. W.; Reed, M. A.; Zhou, C.-W.; Chen, J.; et al. Synthesis and Preliminary Testing of Molecular Wires and Devices. *Chem. - Eur. J.* **2001**, *7*, 5118−5134.

(32) Fan, F.-R. F.; Yang, J.; Cai, L.; Price, D. W.; Dirk, S. M.; Kosynkin, D. V.; Yao, Y.; Rawlett, A. M.; Tour, J. M.; Bard, A. J. Charge Transport Through Self-Assembled Monolayers of Compounds of Interest in Molecular Electronics. *J. Am. Chem. Soc.* **2002**, *124*, 5550−5560.

(33) Chen, J.; Reed, M. A.; Rawlett, A. M.; Tour, J. M. Large On-Off Ratios and Negative Differential Resistance in a Molecular Electronic Device. *Science* **1999**, *286*, 1550−1552.

(34) Lewis, P. A.; Inman, C. E.; Yao, Y.; Tour, J. M.; Hutchison, J. E.; Weiss, P. S. Mediating Stochastic Switching of Single Molecules Using Chemical Functionality. *J. Am. Chem. Soc.* **2004**, *126*, 12214−12215.

(35) Stapleton, J. J.; Harder, P.; Daniel, T. A.; Reinard, M. D.; Yao, Y.; Price, D. W.; Tour, J. M.; Allara, D. L. Self-Assembled Oligo(phenylene-Ethynylene) Molecular Electronic Switch Monolayers on Gold: Structures and Chemical Stability. *Langmuir* **2003**, *19*, 8245−8255.

(36) Donhauser, Z. J.; Mantooth, B. A.; Kelly, K. F.; Bumm, L. A.; Monnell, J. D.; Stapleton, J. J.; Price, D. W.; Rawlett, A. M.; Allara, D.

L.; Tour, J. M.; et al. Conductance Switching in Single Molecules Through Conformational Changes. *Science* **2001**, *292*, 2303−2307.

(37) Guedon, C. M.; Valkenier, H.; Markussen, T.; Thygesen, K. S.; Hummelen, J. C.; van der Molen, S. J. Observation of Quantum Interference in Molecular Charge Transport. *Nat. Nanotechnol.* **2012**, *7*, 305−309.

(38) Fracasso, D.; Valkenier, H.; Hummelen, J. C.; Solomon, G. C.; Chiechi, R. Evidence for Quantum Interference in SAMs of Arylethynylene Thiolates in Tunneling Junctions With Eutectic Ga-In (EGaIn) Top-Contacts. *J. Am. Chem. Soc.* **2011**, *133*, 9556−9563.

(39) Obersteiner, V.; Egger, D. A.; Heimel, G.; Zojer, E. Impact of Collective Electrostatic Effects on Charge Transport Through Molecular Monolayers. *J. Phys. Chem. C* **2014**, *118*, 22395−22401.

(40) Obersteiner, V.; Egger, D. A.; Zojer, E. Impact of Anchoring Groups on Ballistic Transport: Single Molecule vs Monolayer Junctions. *J. Phys. Chem. C* **2015**, *119*, 21198−21208.

(41) Wei, Z.; Hansen, T.; Santella, M.; Wang, X.; Parker, C. R.; Jiang, X.; Li, T.; Glyvradal, M.; Jennum, K.; Glibstrup, E.; et al. Molecular Heterojunctions of Oligo(phenylene Ethynylene)s With Linear to Cruciform Framework. *Adv. Funct. Mater.* **2015**, *25*, 1700−1708.

(42) Kaliginedi, V.; Moreno-García, P.; Valkenier, H.; Hong, W.; García-Suárez, V. M.; Buiter, P.; Otten, J. L. H.; Hummelen, J. C.; Lambert, C. J.; Wandlowski, T. Correlations Between Molecular Structure and Single-Junction Conductance: A Case Study With Oligo(phenylene-Ethynylene)-Type Wires. *J. Am. Chem. Soc.* **2012**, *134*, 5262−5275.

(43) Luo, L.; Choi, S. H.; Frisbie, C. D. Probing Hopping Conduction in Conjugated Molecular Wires Connected to Metal Electrodes. *Chem. Mater.* **2011**, *23*, 631−645.

(44) Tour, J. M. Molecular Electronics. Synthesis and Testing of Components. *Acc. Chem. Res.* **2000**, *33*, 791−804.

(45) Venkataraman, L.; Klare, J. E.; Nuckolls, C.; Hybertsen, M. S.; Steigerwald, M. L. Dependence of Single-Molecule Junction Conductance on Molecular Conformation. *Nature* **2006**, *442*, 904−907.

(46) Maya, F.; Flatt, A. K.; Stewart, M. P.; Shen, D. E.; Tour, J. M. Formation and Analysis of Self-Assembled Monolayers From U-Shaped Oligo(phenylene Ethynylene)s as Candidates for Molecular Electronics. *Chem. Mater.* **2004**, *16*, 2987−2997.

(47) Klare, J. E.; Tulevski, G. S.; Sugo, K.; de Picciotto, A.; White, K. A.; Nuckolls, C. Cruciform Π-Systems for Molecular Electronics Applications. *J. Am. Chem. Soc.* **2003**, *125*, 6030−6031.

(48) Bunz, U. H. F. Poly(aryleneethynylene)s: Syntheses, Properties, Structures, and Applications. *Chem. Rev.* **2000**, *100*, 1605−1644.

(49) Tour, J. M.; Jones, L.; Pearson, D. L.; Lamba, J. J. S.; Burgin, T. P.; Whitesides, G. M.; Allara, D. L.; Parikh, A. N.; Atre, S. Self-Assembled Monolayers and Multilayers of Conjugated Thiols, .Alpha.,.omega.-Dithiols, and Thioacetyl-Containing Adsorbates. Understanding Attachments Between Potential Molecular Wires and Gold Surfaces. *J. Am. Chem. Soc.* **1995**, *117*, 9529−9534.

(50) Weiss, E. A.; Kaufman, G. K.; Kriebel, J. K.; Li, Z.; Schalek, R.; Whitesides, G. M. Si/SiO_2-Templated Formation of Ultraflat Metal Surfaces on Glass, Polymer, and Solder Supports: Their Use as Substrates for Self-Assembled Monolayers. *Langmuir* **2007**, *23*, 9686−9694.

(51) Simmons, J. G. Generalized Formula for the Electric Tunnel Effect Between Similar Electrodes Separated by a Thin Insulating Film. *J. Appl. Phys.* **1963**, *34*, 1793−1803.

(52) Lu, Q.; Liu, K.; Zhang, H.; Du, Z.; Wang, X.; Wang, F. From Tunneling to Hopping: A Comprehensive Investigation of Charge Transport Mechanism in Molecular Junctions Based on Oligo(p-Phenylene Ethynylene)s. *ACS Nano* **2009**, *3*, 3861−3868.

(53) Liu, K.; Li, G.; Wang, X.; Wang, F. Length Dependence of Electron Conduction for Oligo(1,4-Phenylene Ethynylene)s: a Conductive Probe-Atomic Force Microscopy Investigation. *J. Phys. Chem. C* **2008**, *112*, 4342−4349.

(54) Liu, H.; Wang, N.; Zhao, J.; Guo, Y.; Yin, X.; Boey, F. Y. C.; Zhang, H. Length-Dependent Conductance of Molecular Wires and

Contact Resistance in Metal-Molecule-Metal Junctions. *ChemPhysChem* **2008**, *9*, 1416−1424.

(55) Xing, Y.; Park, T.-H.; Venkatramani, R.; Keinan, S.; Beratan, D. N.; Therien, M. J.; Borguet, E. Optimizing Single-Molecule Conductivity of Conjugated Organic Oligomers With Carbodithioate Linkers. *J. Am. Chem. Soc.* **2010**, *132*, 7946−7956.

(56) Sangeeth, C. S. S.; Demissie, A. T.; Yuan, L.; Wang, T.; Frisbie, C. D.; Nijhuis, C. A. Comparison of DC and AC Transport in 1.5−7.5 Nm Oligophenylene Imine Molecular Wires Across Two Junction Platforms: Eutectic Ga-In Versus Conducting Probe Atomic Force Microscope Junctions. *J. Am. Chem. Soc.* **2016**, *138*, 7305−7314.

(57) Wang, W.; Lee, T.; Reed, M. Mechanism of Electron Conduction in Self-Assembled Alkanethiol Monolayer Devices. *Phys. Rev. B: Condens. Matter Mater. Phys.* **2003**, *68*, 035416.

(58) Weiss, E. A.; Chiechi, R. C.; Kaufman, G. K.; Kriebel, J. K.; Li, Z.; Duati, M.; Rampi, M. A.; Whitesides, G. M. Influence of Defects on the Electrical Characteristics of Mercury-Drop Junctions: Self-Assembled Monolayers of N-Alkanethiolates on Rough and Smooth Silver. *J. Am. Chem. Soc.* **2007**, *129*, 4336−4349.

(59) *CRC Handbook of Chemistry and Physics*, 97th ed.; Haynes, W. M., Ed.; CRC Press, 2016.

(60) Doudrick, K.; Liu, S.; Mutunga, E. M.; Klein, K. L.; Damle, V.; Varanasi, K. K.; Rykaczewski, K. Different Shades of Oxide: From Nanoscale Wetting Mechanisms to Contact Printing of Gallium-Based Liquid Metals. *Langmuir* **2014**, *30*, 6867−6877.

(61) Kong, G. D.; Kim, M.; Yoon, H. J. EGaIn Microelectrode for Electrical Characterization of ITO-Based Van Der Waals Interface and Airborne Molecular Contamination of ITO Surface. *J. Electrochem. Soc.* **2015**, *162*, H703−H712.

(62) Ocampo, O. E. C.; Gordiichuk, P.; Catarci, S.; Gautier, D. A.; Herrmann, A.; Chiechi, R. C. Mechanism of Orientation-Dependent Asymmetric Charge Transport In Tunneling Junctions Comprising Photosystem I. *J. Am. Chem. Soc.* **2015**, *137*, 8419−8427.

(63) Garrigues, A. R.; Yuan, L.; Wang, L.; Mucciolo, E. R.; Thompon, D.; del Barco, E.; Nijhuis, C. A. A Single-Level Tunnel Model to Account for Electrical Transport Through Single Molecule- And Self-Assembled Monolayer-Based Junctions. *Sci. Rep.* **2016**, *6*, 26517.